BRAC University Journal, Vol. III, No. 2, 2006, pp. 59-65

FINITE VOLUME METHODS FOR SOLVING HYPERBOLIC PROBLEMS ON EUCLIDEAN MANIFOLDS WITHOUT RADIALLY SYMMETRIC INITIAL CONDITION

Moshiour Rahaman
Department of Mathematics & Natural Science, BRAC University
66 Mohakhali, Dhaka-1212
email:mrahaman@bracuniversity.ac.bd

and

NurHosain Md. Ariful Azim
Department of Business Administration
International Islamic University, Chittagong
email:nhmarif@yahoo.com

ABSTRACT

Many interesting physical systems are successfully modeled with time-dependant conservation laws on smooth manifolds, *M*. Examples of such systems include hydrodynamic flows in non-trivial geometry, important in aerodynamic modeling. Though in many applications the manifold is simply Euclidean space; $M = \nabla^3$, the curvilinear basis on which computes is non-orthogonal and quite complicated. The finite volume methods have very important property of ensuring that basic quantities such as mass, momentum and energy are conserved at a discrete level. Conservation is satisfied over each control volume, over a group of control volumes and over the entire solution domain. The finite volume methods are used to solve conservation laws on Euclidean manifold.

Key words: Finite volume, Conservation, manifold, flux, and wave equations.

I. INTRODUCTION

The most commonly used methods for generating numerical solutions to systems of partial differential equations are based on finite difference methods. A significant limitation of standard finite difference methods is that they usually only produce acceptable results when the evolved solution is sufficiently smooth. This is important because in many applications the models being studied are known to admit solutions in which discontinuities form even for smooth initial data. Much research has been done in the field of computational fluid dynamics into the development of advanced numerical methods, which are capable of accurately evolving solutions irrespective of their smoothness. Finite volume methods achieve this by analyzing a series of Riemann problem for the evolution system and discuss how solutions to Riemann problems can be determined in some basic cases. The numerical simulations carried out in the present work use finite volume methods algorithm of LeVeque (1997). This work is extension of paper M. Rahaman [2]. In the preliminary section, we have discussed tensor, transformation, and manifolds and then go for derivation of conservation laws. We choose finite volume methods for solving conservation law because the methods satisfy conservation property on each domain.

II. PRELIMINARIES

1. Curved manifolds

Differential geometry describes the geometric structure of a curved differentiable manifold, *M*. For example, a manifold *M* may represent the nearly spherical surface of a planet, a curved spacetime in relativity theory. A manifold is a set of points that looks locally Euclidean in that this set can be entirely covered by a collection of local coordinate mappings. Consider a two-dimensional curved manifold that is embedded in ∇^3. Let the coordinates $\left(x^1, x^2\right)$ be the coordinates on the

manifold *M*. This coordinate system can be related to the standard Cartesian coordinate system, (*x, y, z*), through the transformations

$$\left.\begin{aligned} x &= \bar{x}\left(x^1, x^2\right) \\ y &= \bar{y}\left(x^1, x^2\right) \\ z &= \bar{z}\left(x^1, x^2\right) \end{aligned}\right\} \text{ ---------- (1)}$$

A vector, $\left(\mu^1, \mu^2\right)$, in contravariant form on the manifold *M* can be transformed to a vector, $\left(\mu^x, \mu^y, \mu^z\right)$, in Cartesian space through the Jacobian *J* in the following way:

$$\begin{bmatrix} \mu^x \\ \mu^y \\ \mu^z \end{bmatrix} = J \begin{bmatrix} \mu^1 \\ \mu^2 \end{bmatrix} = \begin{bmatrix} \frac{\delta \bar{x}}{\delta x^1} & \frac{\delta \bar{x}}{\delta x^2} \\ \frac{\delta \bar{y}}{\delta x^1} & \frac{\delta \bar{y}}{\delta x^2} \\ \frac{\delta \bar{z}}{\delta x^1} & \frac{\delta \bar{z}}{\delta x^2} \end{bmatrix} \begin{bmatrix} \mu^1 \\ \mu^2 \end{bmatrix} \text{ --------- (2)}$$

Therefore, the coordinate transformations directly give us a natural basis in which to represent vectors on *M*. We will refer to such a basis as a coordinate basis.

2. The metric tensor

The metric tensor, $\overleftrightarrow{g}$, is a symmetric tensor that provides a measure of length on *M*. The metric relates true distances as measured in ∇^3 to the coordinate distances measured in the coordinate system of the manifold. In particular, the line element $ds^2 = (dx)^2 + (dy)^2 + (dz)^2$ in ∇^3 is related to dx^1 and dx^2 through

$$ds^2 = g_{\alpha\beta} dx^\alpha dx^\beta \text{ ---------- (3)}$$

The distance along a curve $C(\lambda)$ parameterized by λ from *C(a)* to *C(b)* is given by

$$L = \int_a^b \left| g_{\alpha\beta} \left(\frac{dx^\alpha}{d\lambda} \right) \left(\frac{dx^\beta}{d\lambda} \right) \right|^{1/2} d\lambda \text{ --------- (4)}$$

The surface area of $\Omega \subseteq M$ can be evaluated by computing the following integral:

$$\text{Surface Area } \Omega = \int_{\Omega\left(x^1, x^2\right)} \sqrt{g}\, dx^1 dx^2 \text{ -------- (5)}$$

where $\sqrt{g}$ is the square root of the determinant of the metric tensor. The components of the tensor $\Gamma^k_{\alpha\beta}$ are referred to as the Christoffel symbols or as connection coefficients. They involve spatial derivatives of the metric tensor $\overleftrightarrow{g}$. In particular, in a coordinate basis they can be written as follows

$$\Gamma^k_{\alpha\beta} = \frac{1}{2} g^{hk} \left(\frac{\delta}{\delta x^\beta} g_{h\alpha} + \frac{\delta}{\delta x^\alpha} g_{h\beta} - \frac{\delta}{\delta x^h} g_{\alpha\beta} \right) \text{ ---(6)}$$

The Christoffel symbols play an important role in wave propagation on curved manifolds.

3. Derivation of conservation laws

Conservation laws are time-dependent systems of partial differential equations (usually non-linear) with a particularly simple structure. In one dimension space the equation take the form:

$$\frac{\partial}{\partial t} q(x,t) + \frac{\partial}{\partial x} f(q(x,t)) = 0 \text{ ---------- (7)}$$

Here $q(x,t) \in R^m$ is an m-dimensional vector of conserved quantities or state variables such as mass, momentum and energy in a fluid dynamics problem. More precisely, q_j is the density function for the jth state variable, with interpretation that $\int_{x_1}^{x_2} q_j(x_j, t)\, dx$ is the total quantity of this state variable in the interval $[x_1, x_2]$ at time *t*.

The fact that these state variables are conserved means that $\int_{-\infty}^{\infty} q_j(x\ , t)\, dx$ should be constant with respect to *t*. The main assumption underlying (7) is that, knowing the value of $q(x,t)$ at a given point and time allows us to determined the rate of flow; or flux of each state variables at (*x,t*). The flux of the *j*th component $f_j(q)$ is called the flux function for the system of conservation laws.

To see how conservation laws arise from physical principles, we begin by driving the equation for conservation of mass in a one dimensional gas dynamics problems; for example flow in a tube where properties of the gas such as density and velocity are assumed to be constant across each cross section of the tube and $\rho(x,t)$ be the density of the gas at point *x* and time *t*. This density is defined in such a way that the total mass of gas in any given section from x_1 to x_2, say, is given by the integral of the density:

Mass in $[x_1, x_2]$ at time $t = \int_{x_1}^{x_2} \rho(x,t)\, dx$. --- (8)

If we assume that the wall of the tube are impermeable and that mass is neither created nor destroyed, then the mass in this one section can change only because of gas flowing across the endpoints x_1 or x_2.

Now let $u(x,t)$ be the velocity of the gas at the point x at time t. Then the rate of flow, or flux of gas past this point is given by:

Mass flux at $(x,t) = \rho(x,t).u(x,t) = q(x,t)$

By our comments above, the rate of change of mass in $[x_1, x_2]$ is given by the difference in fluxes at x_1 and x_2:

$$\frac{d}{dt}\int_{x_1}^{x_2} \rho(x,t)\,dx = q(x_1,t) - q(x_2,t) \quad \text{----- (9)}$$

This is one integral form of the conservation law. Another form is obtained by integrating this in time from t_1 to t_2, giving an expression for the mass in $[x_1, x_2]$ at time $t_2 > t_1$ in terms of the mass at time t_1 and the total flux at each boundary during this period:

$$\int_{x_1}^{x_2} \rho(x,t_2)\,dx - \int_{x_1}^{x_2} \rho(x,t_1)\,dx$$

$$= \int_{t_1}^{t_2} q(x_2,t)\,dt - \int_{t_1}^{t_2} q(x_1,t)\,dt \quad \text{-------- (10)}$$

To derive the differential form of the conservation law; we must now assume that $\rho(x,t)$ *and* $q(x,t)$ are differentiable functions then using,

$$\rho(x,t_2) - \rho(x,t_1) = \int_{t_1}^{t_2} \frac{\partial}{\partial t}\rho(x,t)dt \text{ --(11)}$$

and $q(x_2,t) - q(x_1,t) = \int_{x_1}^{x_2} \frac{\partial}{\partial x} q(x,t)\,dx$ --(12)

Using (11) and (12) in (10) gives:

$$\int_{t_1}^{t_2}\int_{x_1}^{x_2}\left[\frac{\partial}{\partial t}\rho(x,t) + \frac{\partial}{\partial x}q(x,t)\right]dx\,dt = 0 \text{ --(13)}$$

Since this must hold for any section $[x_1, x_2]$ and over any time interval $[t_1, t_2]$ we conclude that in fact the integrand in (13) must be identically zero. That is,

$$\frac{\partial}{\partial t}\rho + \frac{\partial}{\partial x}q = 0 \quad \text{----------(14)}$$

This is the desired differential form of the conservation law for the conservation of mass, which is often called the continuity equation.

4. The Riemann problem

The conservation law together with piecewise constant data having a single discontinuity is known as the Riemann problem. As an example, consider Burger's equation:

$$q_t + qq_x = 0 \quad \text{----------(15)}$$

with piecewise constant initial data:

$$q(x,0) = \begin{cases} q_l \text{ if } x < 0 \\ q_r \text{ if } x > 0 \end{cases} \quad \text{----------(16)}$$

The form of the solution depends on the relation between q_l and q_r.

<u>Case-I:</u> $q_l > q_r$

In this case there is a unique weak solution,

$$q(x,t) = \begin{cases} q_l \text{ if } x < s_t \\ q_r \text{ if } x > s_t \end{cases} \quad \text{----------(17)}$$

where $s_t = \frac{1}{2}(q_l + q_r)$ ----------(18)

is the shock speed, the speed at which the discontinuity travels. Note that characteristics in each of the regions where q is constant go into the shock as time advances.

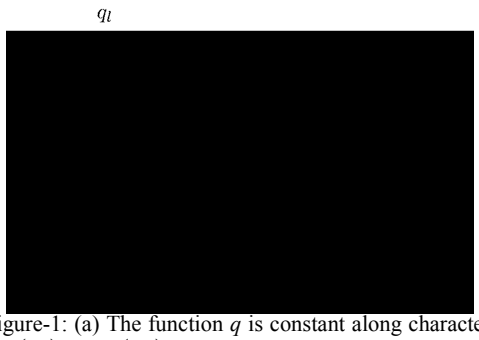

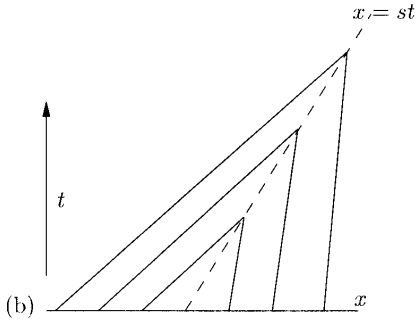

Figure-1: (a) The function q is constant along characteristics. (b) The initial discontinuity in q travels at speed s. Since $f'(q_l) > f'(q_r)$ the characteristics disappear into the line $x = st$.

The speed of propagation can be determined by conservation. The relation between the shock speed s and the states q_l *and* q_r is called the Rankine Hagoniot jumping condition:

$$f(q_l) - f(q_r) = s(q_l - q_r) \quad \text{--------(19)}$$

For scalar problems this gives simply:

$$s = \frac{f(q_l) - f(q_r)}{q_l - q_r} \quad \text{----------(20)}$$

Case-II: $q_l < q_r$

In this case there are infinitely many solutions. One of these is again (17) and (18) in which the discontinuity propagates with speeds. Note that characteristics now go out of the shock and that this solution is not stable to perturbations.

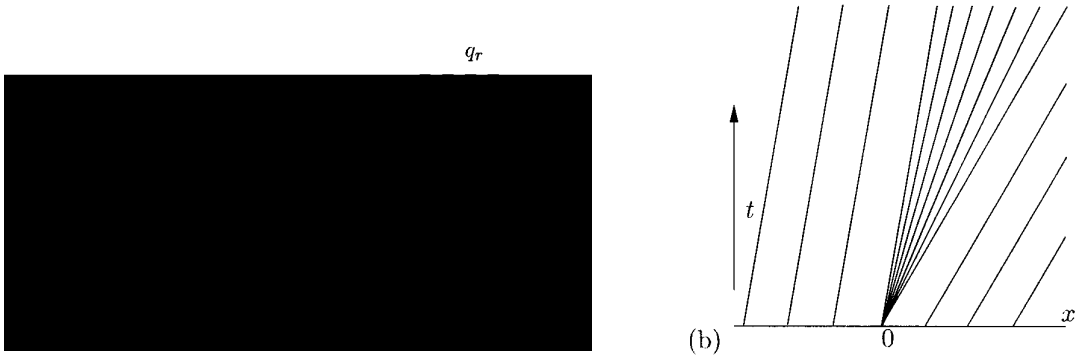

Figure-2: (a) The function q is still constant along characteristics. (b) The initial discontinuity in q now decomposes into a continuously varying rarefaction wave.

If the data is smeared out slightly or if a small amount of viscosity is added to the equation, the solution changes completely.

Another weak solution is the rarefaction wave;

$$q(x,t) = \begin{cases} q_l & if \quad x < q_l t \\ \dfrac{x}{t} & if \quad q_l t \le x \le q_r t \\ q_r & if \quad x > q_r t \end{cases} \quad \text{---------- (21)}$$

This solution is stable to perturbations and is in fact the vanishing viscosity generalized solution.

III. NUMERICAL METHODS

1. Godunov's method

Many methods are based on solving the Riemann problem between the states q_l *and* q_r in order to define the numerical flux $F(q_l, q_r)$. To see how this comes out, it is useful to view the data Q^n at time t_n as defining a piecewise constant function $\overline{q}^n(x,t_n)$ which has the value Q_i^n for all x in the interval C_i. Suppose we could solve the conservation law exactly over the time interval $[t_n, t_{n+1}]$ with initial data $\overline{q}^n(x,t_n)$ called the resulting function $\overline{q}^n(x,t)$ for $t_n \le t \le t_{n+1}$. Then the numerical flux function is defined by

$$F_i^n = \frac{1}{k}\int_{t_n}^{t_{n+1}} f(\overline{q}^n(x_i,t))\,dt \quad \text{---------(22)}$$

Provided that the time step 'k' is small enough, because of the fact that with piecewise constant initial data we can find the exact solution easily by simply piecing together the solutions to each Riemann problem defined by the jump at each interface.

2. Finite volume methods

Rather than viewing Q_i^n as an approximation to the single value $q(x_i,t_n)$, we will now view it as approximating the average value of 'q' over an interval of length $h = \Delta x = \dfrac{b-a}{N}$. We will split the physical domain $[a,b]$ into N intervals denoted by $C_i = [x_i, x_{i+1}]$ where

$x_i = a + (i-1)h$. The value Q_i^n will approximate the average value over the *i*th interval at time t_n which is given by

$$Q_i^n \approx \frac{1}{h}\int_{x_i}^{x_{i+1}} q(x,t_n)\,dx \equiv \frac{1}{h}\int_{C_i} q(x,t_n)\,dx \text{ ----(23)}$$

Notationally it might better to denote the endpoints of the '*i*'th interval by $x_{i-\frac{1}{2}}$ and $x_{i+\frac{1}{2}}$, which would be more symmetric and remind us that Q_i^n is an approximation to the average value between these points. However, the formulas are less cluttered if we stick to integer subscripts.

If $q(x,t)$ is a smooth function, then the integral in (23) agrees with the value of q at the midpoint of the interval to O(h^2). By working with cell averages, however, it is easier to use important properties of the conservation law in deriving numerical methods. In particular, we can insure that the numerical method is conservative in a way that mimics the true solution and this is extremely important in accurately calculating shock waves. This is because $h\sum_{i=1}^{N} Q_i^n$ approximates the integral of q over the entire interval $[a,b]$ and if we use a method that is in conservation form, then this discrete sum will change only due to fluxes at the boundaries $x = a$ and $x = b$. The total mass within the computational domain will be preserved or at least will vary correctly provided the boundary conditions are properly imposed.

The integrand form of the conservation law (10), when applied to one grid cell over a single time step, gives

$$\int_{C_i} q(x,t_{n+1})\,dx - \int_{C_i} q(x,t_n)\,dx = \int_{t_n}^{t_{n+1}} f(q(x_i,t))\,dt - \int_{t_n}^{t_{n+1}} f(q(x_{i+1},t))\,dt$$

Rearranging this and dividing by *h* gives

$$\frac{1}{h}\int_{C_i} q(x,t_{n+1})\,dx = \frac{1}{h}\int_{C_i} q(x,t_n)\,dx - \frac{1}{h}\left[\int_{t_n}^{t_{n+1}} f(q(x_{i+1},t))\,dt - \int_{t_n}^{t_{n+1}} f(q(x_i,t))\,dt\right] \text{-- (24)}$$

This tell us exactly how the cell average of '*q*' from (23) should be updated in one time step. In general, however, we cannot evaluate the time intervals on the right hand side of (24) exactly. Since $q(x_i,t)$ varies with time along each edge of the cell, and we don't have the exact solution to work with. But this does suggest that we should develop numerical method in the flux-differentiating form,

$$Q_i^{n+1} = Q_i^n - \frac{k}{h}(F_{i+1}^n - F_i^n) \text{ ----------(25)}$$

where F_i^n is some approximation to the average flux along $x = x_i$ by using Godunov's method,

$$F_i^n \approx \frac{1}{k}\int_{t_n}^{t_{n+1}} f(q(x_i,t))\,dt \text{ ----------(26)}$$

If we can approximate this average flux based on the values Q^n, then we will have a fully discrete method. Since information propagates with finite speed, it is reasonable to first suppose that we can obtain F_i^n based only on the values Q_{i-1}^n and Q_i^n, the cell averages on either side of this interface. Then we might use a formula of the form.

$$F_i^n = F(Q_{i-1}^n, Q_i^n)$$

Where *F* is some numerical flux function. The method (19) then becomes:

$$Q_i^{n+1} = Q_i^n - \frac{k}{h}\left(F\left(Q_i^n, Q_{i+1}^n\right) - F\left(Q_{i-1}^n, Q_i^n\right)\right) \text{ (27)}$$

The specific method obtained depends on how we choose the formula of *F*, but in general any method of this type is an explicit method with a 3-points stencil. Moreover, it is said to be in conservation form, since it mimics the property (24) of the exact solution. Note that if we sum hQ_i^{n+1} from (19) over any set of cells we obtain:

$$h\sum_{i=1}^{J} Q_i^{n+1} = h\sum_{i=1}^{J} Q_i^n - \frac{k}{h}(F_{j+1}^n - F_I^n) \text{ --- (28)}$$

The sum of the flux differences cancels out except for the fluxes of the extreme edges. Over the full domain we have exact conservation except for fluxes at the boundaries.

Note that (27) can be viewed as a direct finite difference approximation to the conservation law $q_t + f(q)_x = 0$, since rearranging it gives,

$$\frac{Q_i^{n+1} - Q_i^n}{k} + \frac{F(Q_{i+1}^n, Q_i^n) - F(Q_i^n, Q_{i-1}^n)}{h} = 0 \text{ --(29)}$$

Many methods can be equally well viewed as finite difference approximations to this equation or as finite volume methods.

IV. THE SCALAR FIELD EQUATION

We apply the methods for solving hyperbolic equations to the scalar field equation on a Euclidean manifold *M*. This equation models the propagation of acoustic waves in a thin membrane whose shape is given by the manifold *M*. The scalar field equation can be written as:

$$\frac{\partial^2 \delta}{\partial t^2} - \vec{\nabla}(\vec{\nabla}\phi) = 0 \quad \text{----------(30)}$$

The pressure $p(\vec{x},t)$ and the fluid velocity, $u(\vec{x},t)$ can be obtained by taking appropriate temporal and spatial gradients of the scalar field:

$$\left.\begin{aligned} p(\vec{x},t) &= -\frac{\partial}{\partial t}\phi(\vec{x},t) \\ \vec{u}(\vec{x},t) &= \vec{\nabla}\phi(\vec{x},t) \end{aligned}\right\} \quad \text{----------(31)}$$

Replacing $\vec{\phi}(\vec{x},t)$ in equation (30) by the above definitions and imposing that,

$$\vec{\nabla}\left(\frac{\delta\phi}{\delta t}\right) = \frac{\delta}{\delta t}\left(\vec{\nabla}\phi\right) \quad \text{----------(32)}$$

Results in the following system of balance laws for the pressure and the components of the fluid velocity:

$$\frac{\delta q}{\delta t} + \frac{1}{\sqrt{g}}\frac{\delta f^k}{\delta x^k} = \psi_c \quad \text{----------(33)}$$

We investigate the behavior of the methods on three different curvilinear grids that over R^2. The grids used to show a variety of geometric complexity. These grids are defined by the coordinate transformation.

$$x \to x(\xi,\eta) = \alpha\xi + \beta\eta + \theta\xi^2 + \delta\xi\eta$$
$$y \to y(\xi,\eta) = \alpha\eta + \beta\xi + \theta\eta^2 + \delta\xi\eta$$

These grids have been chosen to activate more christoffel symbols as the grid number increases. The third grid has all nonzero christoffel symbols. Only the results for the third grid are presented. The initial pressure pulse has the functional form:

$$P(t=0,x,y) = \begin{cases} a\cos\dfrac{\pi(x'-x_l)}{\delta}+1 & if \ \ |x'-x_l| < \delta \\ 0 & if \ \ |x'-x_l| > \delta \end{cases} \quad (34)$$

Where x_l is taken to be a value in the flat region near the left edge of the grid. This pulse is initialized to be right-propagating. As the wave travels to the right, part of it interacts with the dip of the surface as shown in fig-3. . In this figures, the surfaces is plotted together with the projection of the pressure onto the coordinate plane. They show the time evolution of the pulse as it interacts with the geometry of the dip. First, curves that interact with the edge of the dip converge and cross on the down-wind side of the dip.

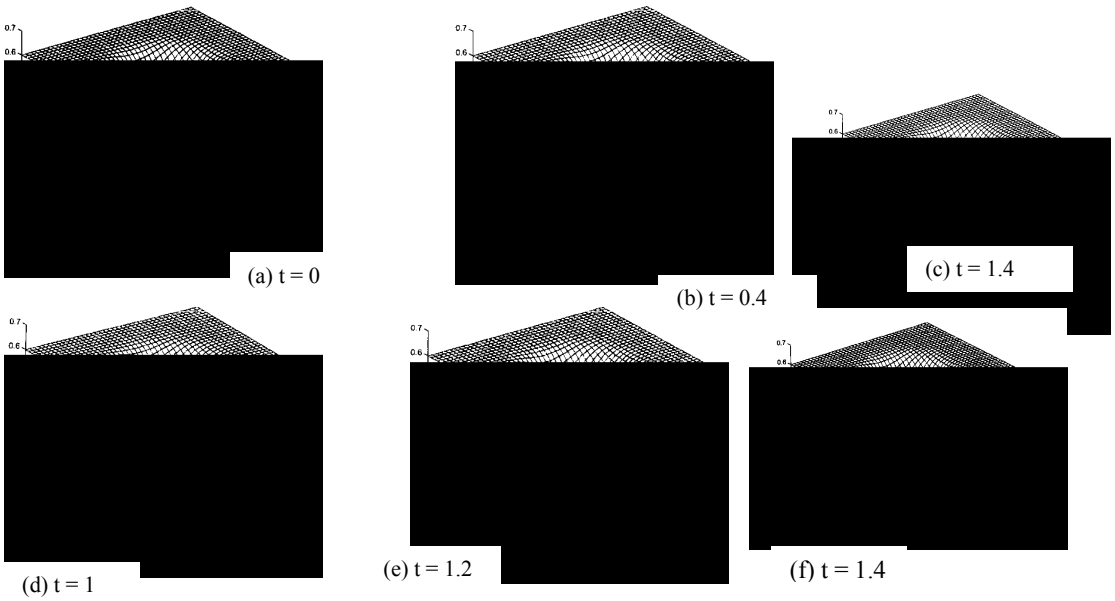

Figure-3: A time sequence of the multidimensional solution. The contours of the solutions are plotted on a plane projected down from the manifold.

Second, curves that interact with the central region of the dip can end up heading in the same direction that they came form. Both of these effects are seen in figures 3.

In figure-3 (c) it appears that the pressure wave is following the geodesics of the surface. In the figures that follow, a small pressure wave begins to travel in the direction from which it comes. Notice that the portion of the wave that does not interact with the geometry continuous on as it would in a Cartesian space.

In order to apply the methods to this problem; equation (30) needs to be cast in the form:

$$\begin{aligned} p_{,t} - v^m_{,m} &= v^m \Gamma^j_{mj} \\ v^k_{,t} - h^{km} p_{,m} &= 0 \end{aligned} \quad \text{---------- (35)}$$

Specifically, on these equations take the form.

$$\left.\begin{aligned} p_{,t} - (v^1)_{,1} - (v^2)_{,2} &= \frac{b_{,1} b_{,11} + b_{,2} b_{,12}}{1 + (b_{,1})^2 + (b_{,2})^2} v^1 + \frac{b_{,2} b_{,22} + b_{,1} b_{,12}}{1 + (b_{,1})^2 + (b_{,2})^2} \\ v^1_{,t} - \left(\frac{1 + (b_{,2})^2}{1 + (b_{,1})^2 + (b_{,2})^2} \right) p_{,1} + \left(\frac{b_{,1} b_{,2}}{1 + (b_{,1})^2 + (b_{,2})^2} \right) p_{,2} &= 0 \\ v^2_{,t} + \left(\frac{b_{,1} b_{,2}}{1 + (b_{,1})^2 + (b_{,2})^2} \right) p_{,1} - \left(\frac{1 + (b_{,1})^2}{1 + (b_{,1})^2 + (b_{,2})^2} \right) p_{,2} &= 0 \end{aligned}\right\} \quad (36)$$

A Riemann solver that can handle the spatially varying functions that appear in the flux for the velocity must be used together with a split method to handle the source term in the pressure equation.

V. CONCLUSIONS

We have presented in this paper finite volume methods for hyperbolic partial differential equations on Euclidean manifolds. The equation is solved without radially symmetric initial condition (34) in a coordinate basis resulting from the choice of coordinates on the manifold. The claim is verified by using the finite volume algorithm to compute the solution to the scalar field hyperbolic partial differential equations on Euclidean manifold. The Fortran code that is used to obtain the solution by using the standard clawpack software package.

REFERENCES

[1] R.J. LeVeque. Finite Volume Methods for Hyperbolic Problems. Cambridge University Press, 2002.

[2] Moshiour Rahaman. Finite volume methods for solving Hyperbolic partial differential equations on Curved manifolds. BRAC University Journal, Vol. II, No. 1, 2005, pp. 99-103

[3] J.M. Bardeen and L.T. Buchman. Numerical tests of evolution systems, gauge conditions, and boundary conditions for 1d colliding gravitational plane waves. Phys. Rev. D, 65, 2002.

[4] J.Y-K. Cho and L.M. Polvani. The emergence of jets and vortices in freely evolving, shallow-water turbulence on a sphere. Physics of Fluids, 8:1531–1552, 1995.

[5] J.A. Font. Numerical hydrodynamics in general relativity. Living Rev. Rel., 2000.

[6] A. Harten and J.M. Hyman. Self-adjusting grid methods for one-dimensional hyperbolic conservation laws. J. Comp. Phys., 50:235–269, 1983.

[7] R. Heikes and D.A. Randall. Numerical integration of the shallow water equations on a twisted icosahedral grid. Part I: Basic design and results of tests. Monthly Weather Review, 123:1862–1880, 1995.

[8] R. Heikes and D.A. Randall. Numerical integration integration of the shallow water equations on a twisted icosahedral grid. Part II: A detailed description of the grid and an analysis of numerical accuracy. Monthly Weather Review, 123:1881–1887, 1995.

[9] C. Helzel. Numerical approximation of conservation laws with stiff source terms for the modelling of detonation waves. PhD thesis, Otto-von-Guericke-Universit¨at Magdeburg, Magdeburg,Germany, 2000.

[11] J. Kevorkian. Partial Differential Equations: Analytic Solution Techniques. Springer-Verlag, New York, second edition, 2000.

[12] J.O. Langseth and R.J. LeVeque. A wave propagation method for three-dimensional hyperbolic conservation laws. J. Comp. Phys., 165:126–166, 2000.

[13] Wulf Rossman. Lecture notes on Differential Geometry.

[14] J.M. Martý and E. Muller. Numerical hydrodynamics in special relativity. Living Rev. in Rel., 1999.